TOPTIER CNS Summer School 2026

POTENTIAL-MODEL STUDY OF EARLY-UNIVERSE RADIATIVE CAPTURE REACTIONS AND ASTROPHYSICAL IMPLICATIONS

Dao Nhut Anh

Ho Chi Minh City University of Education, Vietnam

Daejeon, August 25, 2026

Stellar evolution

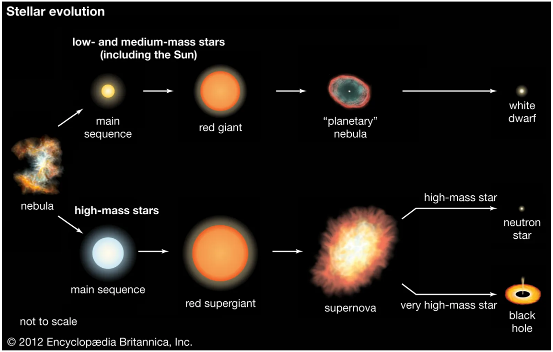

Figure 1: Stellar evolution

- **Stellar nucleosynthesis** operates over **billions of years** in high-density environments with a low photon-to-baryon ratio.
- **Hydrogen burning** via the **pp-chain** and **CNO cycle** converts H into He, releasing energy to maintain hydrostatic equilibrium against gravity.

Big Bang Nucleosynthesis (BBN)

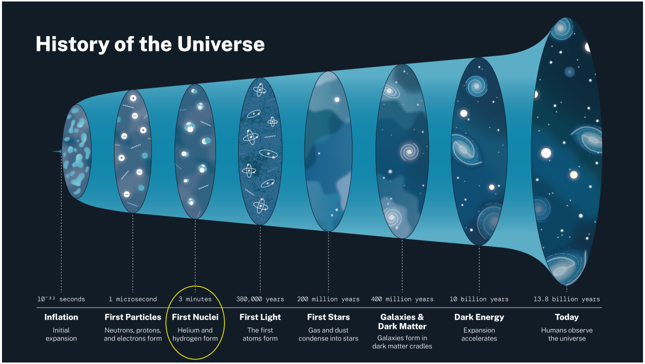

Figure 2: History of the Universe. BBN started from 3 minutes after Big Bang

- **Production of nuclei** other than H from **3 minutes** after Big Bang.
- **BBN** started with the work of Gamow, Alpher, and Herman in the 1940s, who predicted a connection between the elements' formation and the cosmic background radiation.

Formation of light elements

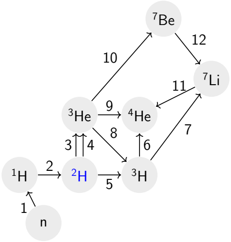

1. $\mathrm{n} \to {}^1\mathrm{H} + e^- + \bar{\nu}$
2. ${}^1\mathrm{H} + \mathrm{n} \to {}^2\mathrm{H} + \gamma$
3. ${}^2\mathrm{H} + {}^1\mathrm{H} \to {}^3\mathrm{He} + \gamma$
4. ${}^2\mathrm{H} + {}^2\mathrm{H} \to {}^3\mathrm{He} + \mathrm{n}$
5. ${}^2\mathrm{H} + {}^2\mathrm{H} \to {}^3\mathrm{H} + {}^1\mathrm{H}$
6. ${}^2\mathrm{H} + {}^3\mathrm{H} \to {}^4\mathrm{He} + \mathrm{n}$
7. ${}^3\mathrm{H} + {}^4\mathrm{He} \to {}^7\mathrm{Li} + \gamma$
8. ${}^3\mathrm{He} + \mathrm{n} \to {}^3\mathrm{H} + {}^1\mathrm{H}$
9. ${}^3\mathrm{He} + {}^2\mathrm{H} \to {}^4\mathrm{He} + {}^1\mathrm{H}$
10. ${}^3\mathrm{He} + {}^4\mathrm{He} \to {}^7\mathrm{Be} + \gamma$
11. ${}^7\mathrm{Li} + {}^1\mathrm{H} \to {}^4\mathrm{He} + {}^4\mathrm{He}$
12. ${}^7\mathrm{Be} + \mathrm{n} \to {}^7\mathrm{Li} + {}^1\mathrm{H}$

Figure 3: Big Bang Nucleosynthesis (BBN)

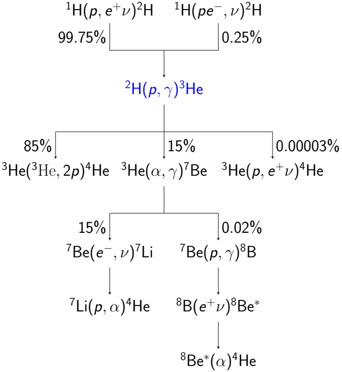

Figure 4: Proton-proton chain

- $p(n,\gamma)d$ and $d(p,\gamma)^3$He play a vital role in deuterium's formation and destruction. [N. L. Anh, **D. N. Anh**, D. H. Tho, N. H, Nha, *Physica Scripta* 599 (2024)]

Overview

1. $p(n,\gamma)d$ and $d(p,\gamma)^3$He:
   - **In Experiment:** LUNA collaboration [*Casella et al.*, **Nuclear Physics A** 706 (2002), *Mossa et al.*, **Nature** 587 (2020)], *Suzuki et al.*, **Astrophysics Journal Letter** 439 (1996), *Nagai et al.*, **Physical Review C** 56 (1997)
   - **In theory:** *Marcucci et al.*, **Physical Review Letters** 116 (2016): *ab initio* calculation; *Acharya et al.*, **Physics Letters B** 827 (2022): χEFT calculation
2. $[\mathrm{D/H}]$ ratio:
   - **In Experiment:** *Mossa et al.*, **Nature** 587 (2020), *Cooke et al.*, **The Astrophysical Journal** 102 (2018)
   - **In Theory:** *Coc et al.*, **Physical Review D** 92 (2015): Kawano BBN code
3. **This work:** Calculating the [D/H] ratio of BBN using `PArthENoPE` code (3 versions).
   - Pisanti *et al.*, Computer Physics Communications, 178 (2008).
   - Consiglio *et al.*, Computer Physics Communications, 233 (2018).
   - Gariazzo *et al.*, Computer Physics Communications, 271 (2022).

Procedure

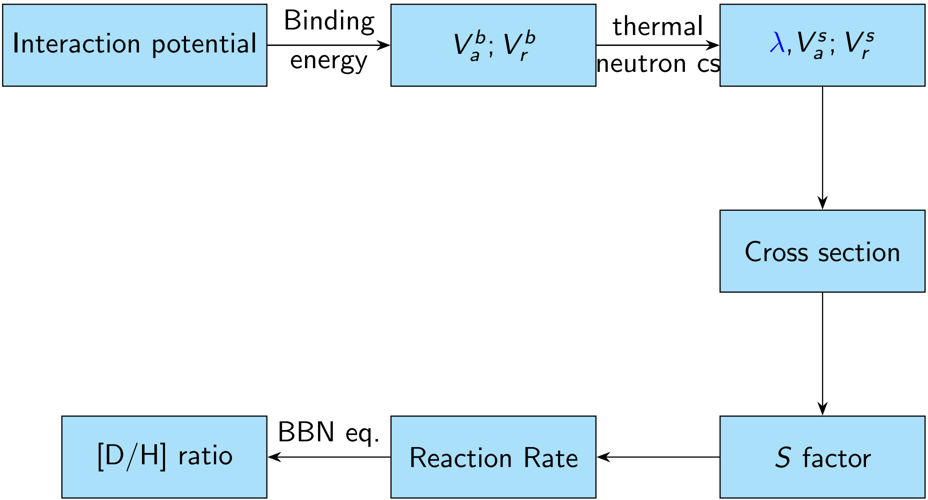

Figure 5: Procedure for calculating primordial deuterium abundance

Physical quantities will be used in calculations

Baryon-to-photon ratio

$$\eta_{10} = 10^{10} \times \frac{n_B}{n_\gamma}. \tag{1}$$

Primordial abundance

$$X_i = \frac{n_i}{n_B}, \qquad i = n, p, d \tag{2}$$

D/H ratio

$$\frac{D}{H} = \frac{X_D}{X_H} = \frac{n_D}{n_H} \tag{3}$$

Energy density of baryons

$$\rho_B = \left[M_u + \sum_i \left(\Delta M_i + \frac{3}{2} T \right) X_i \right] n_B. \tag{4}$$

Pressure of baryons

$$p_B = T n_B \sum_i X_i \tag{5}$$

The set of differential equations in the theory of BBN

Friedmann equation

$$\frac{\dot{a}}{a} = H = \sqrt{\frac{8\pi G_N}{3}\rho}. \tag{6}$$

Baryon conservation

$$\frac{\dot{n}_B}{n_B} = -3H. \tag{7}$$

Energy conservation

$$\dot{\rho} = -3H(\rho + p). \tag{8}$$

Boltzmann equation

$$\dot{X}_i = \sum_{j,k,l} N_i \left[R_{kl\to ij}(T)\frac{X_l^{N_l} X_k^{N_k}}{N_l!N_k!} - R_{ij\to kl}(T)\frac{X_i^{N_i} X_j^{N_j}}{N_i!N_j!} \right]. \tag{9}$$

The Universe charge neutrality

$$n_B \sum_j Z_j X_j = n_{e^-} - n_{e^+} = T^3 L\left(\frac{m_e}{T}, \phi_e\right). \tag{10}$$

Solve those equations to find **Deuterium-to-hydrogen ratio [D/H]**

Reaction rate

Nuclear reaction rate

$$R(T) = \left(\frac{8}{\pi\mu}\right)^{1/2} \frac{N_A}{(k_B T)^{3/2}} \int S(E)\exp(-2\pi\eta)\exp\left(-\frac{E}{k_B T}\right) dE.$$

$R(T)$ can be approximated analytically [Serpical P et al., *J. Cosmol. Astropart. Phys.* 010 (2004), Pisanti O et al., *J. Cosmol. Astropart. Phys.* 020 (2021)]

$$R_{\rm png} \approx a_0 \left(1 + \sum_{i=1}^{6} a_i T^{i/2}\right), \tag{11}$$

$$R_{\rm dpg} \approx T^{-2/3} \exp\left(-\frac{a_0}{T^{1/3}}\right) \sum_{i=0}^{17} a_{i+1} T^{i/3}. \tag{12}$$

Cross section

Astrophysical S factor

$$S(E) = E \exp(2\pi\eta)\sigma(E). \tag{13}$$

Radiative capture cross section

$$\sigma_{n\ell_f j_f J_f}(E) = \frac{4}{3}\frac{1}{\hbar v}\left(\frac{4\pi}{3}k_\gamma^3\right)\frac{1}{(2S_P+1)(2S_T+1)}(|M_{E1}|^2 + |M_{M1}|^2). \tag{14}$$

Reduced matrix elements of the $\Omega 1$ transition

$$M_{\Omega 1} = \langle [S_T \otimes (\ell_f \otimes S_P)_{j_f}]_{J_f} || \mathcal{O}_{\Omega 1} || [S_T \otimes (\ell_i \otimes S_P)_{j_i}]_{J_i} \rangle \tag{15}$$

Interaction potential

Phenomenological potential model

$$V(r) = V_{\mathrm{MT}} + V_{\mathrm{C}}(r). \tag{16}$$

Malfliet-Tjon term [Malfliet, R.A., J. A. Tjon, NPA 127(1) (1969)]

$$V_{\mathrm{MT}}(r) = V_r \frac{e^{-\mu_r r}}{r} - V_a \frac{e^{-\mu_a r}}{r}, \tag{17}$$

$$V^s_{\mathrm{MT}}(r) = \lambda V^b_{\mathrm{MT}}(r). \tag{18}$$

Table 1: Parameters of the bound (b) potentials

Reaction	r_0 [fm]	μ_r [fm^{-1}]	V_r^b [MeV]	μ_a [fm^{-1}]	V_a^b [MeV]
$p(n,\gamma)$	2.506	3.11	1458	1.55	632
$d(p,\gamma)$	2.831	3.11	1458	1.55	632

Coulomb term

$$V_{\mathrm{C}}(r) = \begin{cases} \dfrac{Z_P Z_T e^2}{2r_0}\left(3 - \dfrac{r^2}{r_0^2}\right), & r < r_0 \\ \dfrac{Z_P Z_T e^2}{r}, & r \geqslant r_0 \end{cases} \tag{19}$$

Impulse approximation for nuclear scattering potential

$$V^s_{pd} = V^s_{pn} + V^s_{pp} = 2V^s_{pn} \tag{20}$$

Cross section of $p(n,\gamma)$ reaction

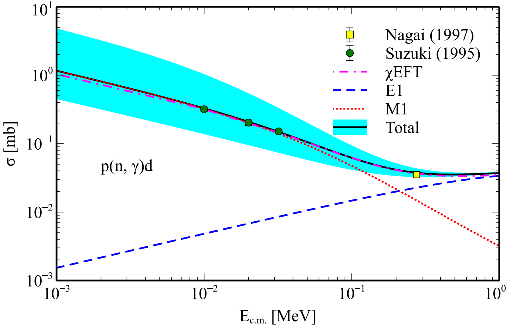

Figure 6: Cross section of $p(n,\gamma)$ reaction below 1 MeV [N. L. Anh, **D. N. Anh**, H. T. An, N. G. Huy, B. M. Loc, *Physica Scripta*, 101 (2026)].

- $\lambda_{\mathrm{png}} = 0.734 \pm 0.023$ (constrained by the thermal neutron capture c.s $\sigma_n = 332.6 \pm 0.7$ mb and Nagai's data point)
- The small experimental uncertainty translates into a tight constraint on the λ
- Below 100 keV, the $M1$ transition dominates.

Astrophysical S factor of $d(p, \gamma)$ reaction

- $\lambda_{\rm dpg} = 2\lambda_{\rm png} = 1.470 \pm 0.046$ ($V_{pd} = V_{np} + V_{pp} = 2V_{np}$)
- $S(E) \approx 0.228 + 5.946E + 7.929E^2 - 3.145E^3$ eVb

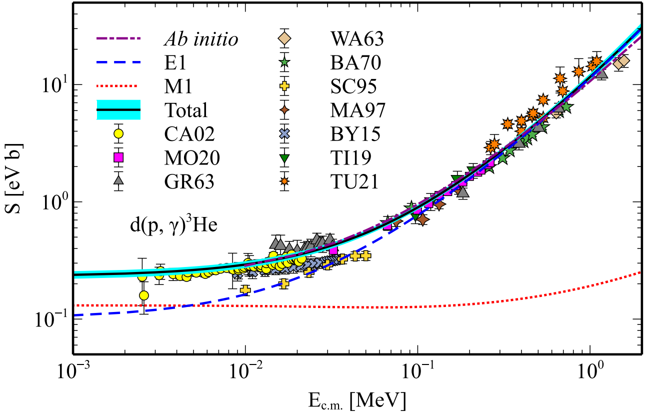

Figure 7: Astrophysical S factor of $d(p, \gamma)$ reaction below 2 MeV [N. L. Anh, **D. N. Anh**, H. T. An, N. G. Huy, B. M. Loc, *Physica Scripta*, 101 (2026)].

[D/H] ratio

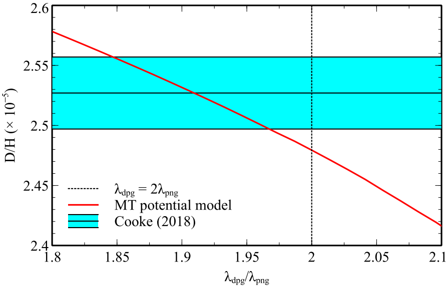

Figure 8: D/H as a function of the ratio $\lambda_{\rm dpg}/\lambda_{\rm png}$ obtained in the present work [N. L. Anh, **D. N. Anh**, H. T. An, N. G. Huy, B. M. Loc, *Physica Scripta*, 101 (2026)].

Table 2: D/H abundance ratio from BBN prediction and observation [N. L. Anh, **D. N. Anh**, H. T. An, N. G. Huy, B. M. Loc, *Physica Scripta*, 101 (2026)].

References	D/H ($\times 10^{-5}$)
Cooke *et al.* (2018)	2.527 ± 0.030
Mossa *et al.* (2020)	2.52 ± 0.09
Pitrou *et al.* (2021)	2.439 ± 0.037
Pisanti *et al.* (2021)	2.51 ± 0.07
Yeh *et al.* (2021)	2.51 ± 0.11
Shen & He (2024)	2.471 ± 0.039
Launders *et al.* (2026)	2.442 ± 0.040
This work	$2.479^{+0.350}_{-0.177}$

Comparison of primordial light-element abundances

Table 3: Comparison of primordial light-element abundances obtained using different radiative-capture rate inputs [N. L. Anh, **D. N. Anh**, H. T. An, N. G. Huy, B. M. Loc, *Physica Scripta*, 101 (2026)].

Abundances	Obs.	Ando *et al.* (2006)	Johnson *et al.* (2001)	Potential model
Y_p	0.2449	0.24852	0.24849	$0.24683^{+0.0005}_{-0.0007}$
$\mathrm{D/H}$ $(\times 10^{-5})$	2.527	2.5467	2.5580	$2.4794^{+0.3500}_{-0.1773}$
$^{3}\mathrm{He/H}$ $(\times 10^{-6})$	< 11	10.0921	10.0864	$10.4947^{+0.3894}_{-0.6199}$
$^{7}\mathrm{Li/H}$ $(\times 10^{-10})$	1.58	4.4646	4.3632	$4.7217^{+4.4313}_{-2.8554}$

The predicted primordial abundances are sensitive to the adopted $p(n,\gamma)$ and $d(p,\gamma)$ reaction rates.

Conclusions

Summary

- A consistent Malfliet-Tjon potential-model framework describes both $p(n,\gamma)$ and $d(p,\gamma)$ within a common low-energy scattering dynamics, including $E1$ and $M1$ transitions.
- The model reproduces the available low-energy capture data and yields a primordial abundance $\mathrm{D/H} = 2.479^{+0.177}_{-0.350} \times 10^{-5}$, consistent with observations and recent BBN calculations.
- The uncertainty in $\mathrm{D/H}$ is propagated from the low-energy scattering dynamics through the scaling factor λ, constrained by the thermal $p(n,\gamma)$ cross section.

Outlook

- Develop a more microscopic unified description of $p(n,\gamma)$ and $d(p,\gamma)$ using realistic nucleon-nucleon interactions.
- Investigate the validity of the impulse approximation for the effective pd interaction.

Thank you for your attention!

Nucleosynthesis

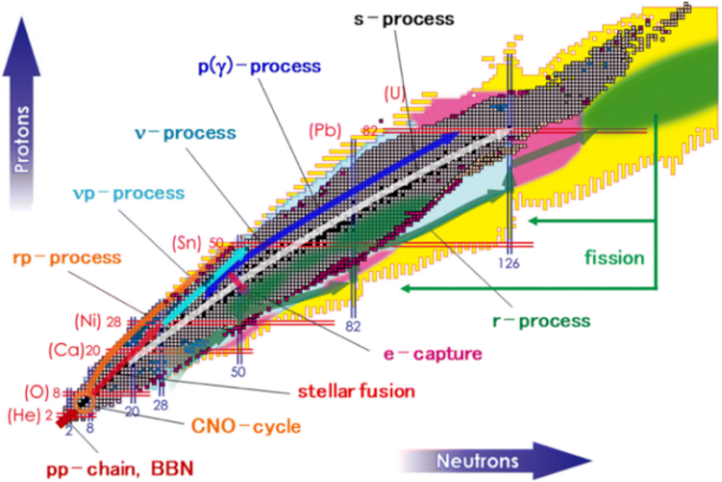

Figure 9: Nucleosynthesis. There is a wide range of complicated processes. The reactions compete with each other.

Radiative capture reaction

Radiative capture reaction: an electromagnetic transition from the **scattering state** to **bound state**. For example, proton radiative capture

$$p + A \to B + \gamma, \qquad \text{or} \qquad A(\mathrm{p}, \gamma)B$$

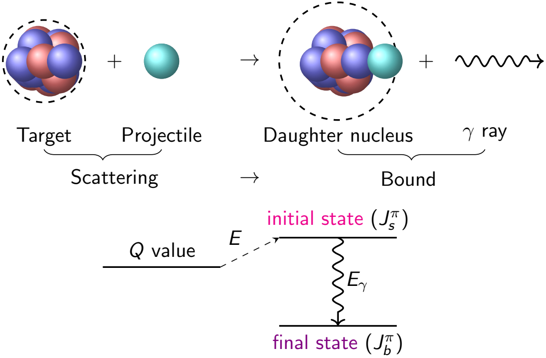

Figure 10: Diagram of the radiative capture process.

Astrophysical S factor of radiative capture

The astrophysical S **factor** is defined by

$$S(E) = E \exp(2\pi\eta)\sigma(E).$$

Gamow window function

$$g(E) = \exp\left[-\frac{E}{k_B T} - 2\pi\eta(E)\right]$$

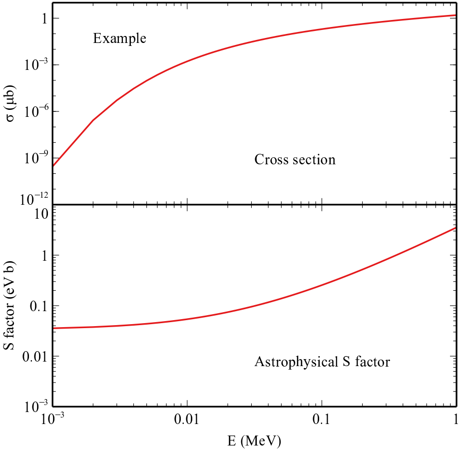

Figure 11: Cross section of **charged-particle capture** drops rapidly at low energy.

$E1$ transition

$E1$ transition operator

$$\mathcal{O}_{E1} = C_e r Y_1^{\mu}$$

Effective charge

$$C_e = \frac{Z_P}{m_P} - \frac{Z_T}{m_T}$$

$E1$ transition matrix element

$$M_{E1} = C_e \sqrt{\frac{3}{4\pi}} (-1)^{S_T + j_f + J_i + 1} \hat{J}_i \hat{J}_f \left\{ \begin{array}{ccc} j_f & J_f & S_T \\ J_i & j_i & 1 \end{array} \right\} M_{0,E1}^{(\mathrm{s.p.})}$$

Hat notation

$$\hat{J} = \sqrt{2J+1}$$

Wigner $6j$ coefficient

$$\left\{ \begin{array}{ccc} j_f & J_f & S_T \\ J_i & j_i & 1 \end{array} \right\}$$

$M1$ transition

$M1$ transition operator

$$\mathcal{O}_{M1} = \sqrt{\frac{3}{4\pi}} \left(C_m \hat{\ell}_\mu + 2\mu_P \hat{S}_{P,\mu} + 2\mu_T \hat{S}_{T,\mu} \right)$$

Effective magnetic moment $C_m = \left(Z_P/m_P^2 + Z_T/m_T^2 \right) m\mu_N$

$M1$ transition matrix element

$$M_{M1} = \sqrt{\frac{3}{4\pi}} \left(M_{M1}^{(0)} + M_{M1}^{(1)} + M_{M1}^{(2)} \right)$$

in which

$$M_{M1}^{(0)} = C_m (-1)^{S_T + j_i + J_f + 1} \hat{j}_i \hat{J}_f \begin{Bmatrix} j_f & J_f & S_T \\ J_i & j_i & 1 \end{Bmatrix} M_{0,M1}^{(\mathrm{s.p.})}$$

$$M_{M1}^{(1)} = \mu_P (-1)^{S_T + j_i + J_f + 1} \hat{J}_i \hat{J}_f \begin{Bmatrix} j_f & J_f & S_T \\ J_i & j_i & 1 \end{Bmatrix} M_{1,M1}^{(\mathrm{s.p.})}$$

$$M_{M1}^{(2)} = \mu_T \delta_{j_i j_f} (-1)^{S_T + j_f + J_i + 1} \hat{J}_i \hat{J}_f \begin{Bmatrix} S_T & J_i & j_f \\ J_f & S_T & 1 \end{Bmatrix} \hat{S}_T \tilde{S}_T M_{2,M1}^{(\mathrm{s.p.})}$$

with $\tilde{S}_T = \sqrt{S_T(S_T+1)}$.

Single particle reduced matrix element

Single particle reduced matrix element

$$M^{(\mathrm{s.p.})}_{i,\Omega 1} = A_{i,\Omega 1} \cdot I_{\Omega 1}$$

Geometrical coefficients

$$A^{(\mathrm{s.p.})}_{0,E1} = \hat{j}_f \hat{\ell}_f \hat{\ell}_i \begin{pmatrix} \ell_f & 1 & \ell_i \\ 0 & 0 & 0 \end{pmatrix} \begin{Bmatrix} \ell_f & j_f & S_P \\ j_i & \ell_i & 1 \end{Bmatrix}$$

$$A^{(\mathrm{s.p.})}_{0,M1} = \delta_{\ell_i \ell_f} (-1)^{\ell_f + S_P + j_i + 1} \hat{j}_i \hat{j}_f \begin{Bmatrix} \ell_f & j_f & S_P \\ j_i & \ell_i & 1 \end{Bmatrix} \hat{\ell}_i \tilde{\ell}_i$$

$$A^{(\mathrm{s.p.})}_{1,M1} = \delta_{\ell_i \ell_f} (-1)^{\ell_i + S_P + j_f + 1} \hat{j}_i \hat{j}_f \begin{Bmatrix} S_P & j_f & \ell_i \\ j_i & S_P & 1 \end{Bmatrix} \hat{S}_P \tilde{S}_P$$

$$A^{(\mathrm{s.p.})}_{2,M1} = \delta_{\ell_i \ell_f} \delta_{j_i j_f}$$

Radial overlap integrals of two states

$$I_{E1} = \int \phi_{n\ell_f j_f}(r) \chi_{\ell_i j_i}(E, r) r \, dr,$$

$$I_{M1} = \int \phi_{n\ell_f j_f}(r) \chi_{\ell_i j_i}(E, r) \, dr.$$

Reaction rates and light-element abundances

Table 4: Coefficients a_i used in the analytical reaction-rate parametrizations [Le Anh et al., *Physica Scripta*, 101 (2026)].

$p(n,\gamma)$			
i	a_i	i	a_i
0	46384.1755	4	−0.3858
1	−0.5396	5	0.0778
2	−0.3765	6	−0.0058
3	0.7870		

$d(p,\gamma)$			
i	a_i	i	a_i
0	4.9476	10	−84.6097
1	−209.4585	11	−37687.4043
2	497230.8185	12	66.8863
3	−1460914.9799	13	51.1938
4	1448197.8718	14	8614.1906
5	−625.3102	15	−41.0109
6	−620950.9505	16	−3805.1857
7	517.9641	17	1574.4794
8	222848.7887	18	−193.3532
9	−0.0000		